

Guosong Zhang^{1*}, Jens M. Hovem^{1,2}, Hefeng Dong¹, Tor A. Reinen²

¹ *Norwegian University of Science and Technology, Trondheim 7491, Norway*

² *SINTEF, SINTEF-ICT, Strindveien 4, Trondheim 7465, Norway*

A design for timing pulse acquisition in underwater multipath environments

Received 03.08.2009, published 17.09.2009

A design is proposed for acoustic timing pulse acquisition, and it is suitable for uses in reverberant multipath environments. This scheme uses two identical broadband pulses for timing, and it is motivated by passive phase conjugation. It is simple in signal processing. The first pulse is used as a probe pulse to estimate the channel impulse response, and then the received probe replaces the replica signal later to catch the second pulse. Within coherence time, a fixed threshold can be preset. A detector makes a decision on the correlation coefficient between the first pulse and the second one, as the coefficient has a great immunity to channel impulse response. In this way, it is easy and robust for receivers to realize acquisition. It shows advantages for independent receivers operating in the shallow water channel.

Keywords: acquisition, threshold, timing correlation, passive phase conjugation

INTRODUCTION

The underwater acoustic (UWA) signals are subject to time-varying multipath [1], which depends on source/receiver configurations and environmental conditions. Broadband signals with good auto-correlation properties are frequently used as preamble pulses for time synchronization, for example linear modulation frequency waveform. Replica-correlator in receivers is often used to match-filtering the preamble pulses for timing. The waveform is important for acquisition in underwater applications, as the channel is more complicated than radio channel. It is designed to be of good auto-correlation, which has narrow main lobe and low side lobes in order to make a decision with high acquisition probability. Xiaoyi Hu [2] shows little how to realize acquisition in multipath environments, as time-varying multipath interferes detection. The method in [3] is limited in orthogonal frequency division multiplexing (OFDM) technique. J. Rice and D. Green [4] adopt combination waveforms, hyperbolic frequency modulation (HFM) and tones, for precise time synchronization under Doppler spread. Doppler estimations from tones are used to compensate timing errors, and they discuss little how to overcome multipath interference. The acquisition of timing pulse is a significant part of numerous applications both in air and water, such as underwater ranging and communication. It provides timing information for the receivers [5]

In many long-term deployed subsea platforms, the receivers need to operate independently and automatically with as little assistance as possible from technicians of high cost, and it is

* Corresponding author, e-mail: Guosong@iet.ntnu.no

better for the receivers to operate under most channel conditions. The UWA channel has its own characteristics [6]. There is reverberant multipath due to reflections and refractions as well as Doppler spread because of relative movement. Besides, a high attenuation from absorption and spreading is also a negative factor. Overlapped multipath in propagation with different Doppler shifts deteriorates the performance of match-filter. The replica signal is totally different from the received signal in multipath channel, and there are peaks in correlation output. The peaks confuse detector's automatic determination on acquisition (Figure 1), and let alone slow time-varying magnitudes of multipath. For randomly deployed receivers, they are unable to reconstruct a replica signal as exactly as that they will receive, which is in order to optimize match-filtering, as they have little information about channel configurations.

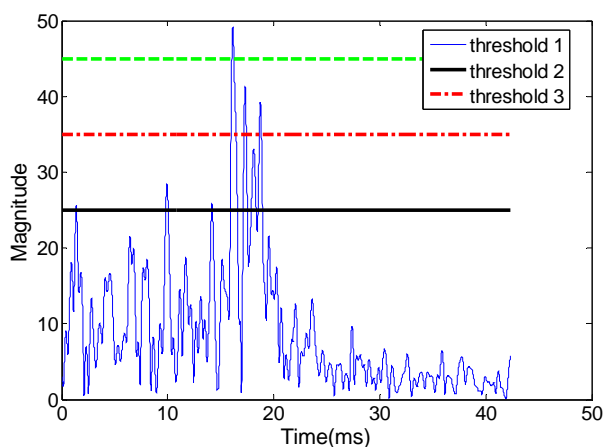


Figure 1.

The acquisition time of the timing pulse using a simple threshold technique changes with different preset magnitude thresholds, and it worsens with multipath

In an effort to develop a reliable and feasible acquisition method for receivers, the design of using two identical broadband preambles for acquisition is proposed, which are aligned apart within coherence time. The signal processing for receivers is given, and it is based on passive phase conjugation (PPC). This design focuses on realization but not waveform designs. It realizes acquisition based on detecting a correlation coefficient between two pulses, as the coefficient is less affected by the multipath resulted from acoustic propagation. It is not computational intensive and complicated in signal processing. These advantages are valuable for independent receivers. Field trials data are analyzed to show acquisition difficulties by match-filtering and our improvements, and the results support the feasibility of this design.

1. EXPERIMENTS AND ANALYSIS

Timing pulses are designed according to their ambiguity functions, so broadband signals of good time compression characteristics are often chosen as the preamble pulses for time recovery for receivers, such as transponders and active sonar systems. HFM, Linear frequency modulation (LFM), and maximum-length sequence spreading waveforms are frequently adopted, and the last two waveforms were tested in lake and sea experiments respectively.

The lake experiment was carried out in free drift, a LFM signal of 100 ms duration was repetitively transmitted with a period of 200 ms for around 1 minute. Water depth in the experimental area is about 30 m. The hemispherical directional source projector and the hydrophone were located at 1.5 m below the surface, and they are separated by a distance of 1 km. The LFM signal was centered at 8.6 kHz with a bandwidth of 5 kHz.

Time changing channel impulse response (CIR) estimated by the periodical LFM signals is noticed as shown in Figure 2. The CIR estimations are not aligned in time, which is resulted from Doppler spread. Doppler spread is caused by relative movement between the transmitter and the receiver. Comparing the received signal with the original transmitted signal [7], there is compression or dilation in time duration [8], which is due to low acoustic propagation speed. There are strong paths that could be detected, and slow time-varying multipath makes it difficult for acquisition based on a fixed magnitude threshold. For example, the maximum magnitudes change nearly 3 dB from the beginning to the end shown in Figure 2. To random deployed receivers, for example acoustic modems, those changes bring difficulties for automatic acquisition with a fixed threshold. Even in the stationary sea experiment, magnitude changes caused by time-varying multipath are noticed.

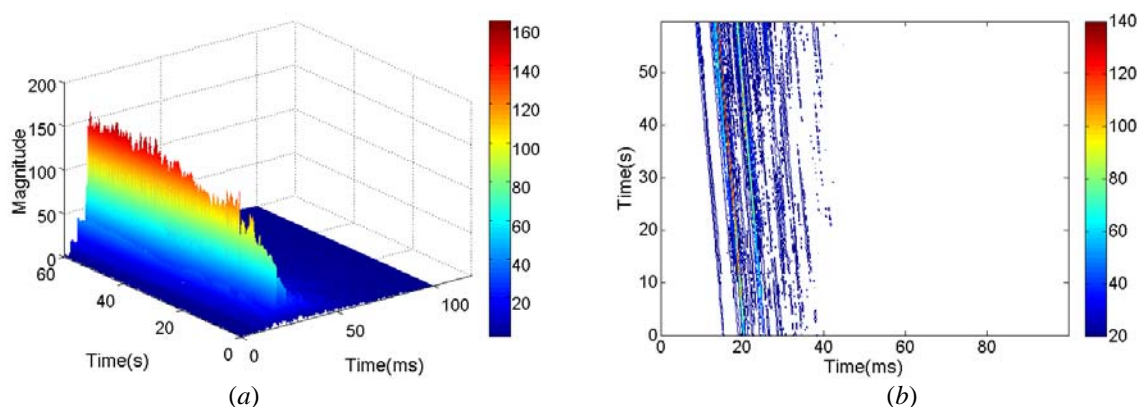


Figure 2. CIRs are estimated by replica correlation in 1 minute, and correlation magnitudes are shown in 3-dimension (a) and contour (b)

The sea trial was carried out in a stationary scenario on November 2, 2007 in Trondheim harbor, Norway (Figure. 3). The direct-sequence spread-spectrum (DSSS) signals were consecutively transmitted for 1 minute. The DSSS signals were centered at 38 kHz with a bandwidth of 3 kHz. The transmitted symbols were spread with a maximum-length sequence of 127 chips, which was modulated using binary phase shift-keying, and each symbol had a time duration of 42.3 ms. One transmitter with a directional projector was deployed at depth of 2 m. Two identical receivers of RxA and RxB recorded the received signals, they are separated vertically by 0.43 m, and RxA is the upper one 2 m below the sea surface. The receivers and the transmitter used directional transducers of 10 degrees beam width.

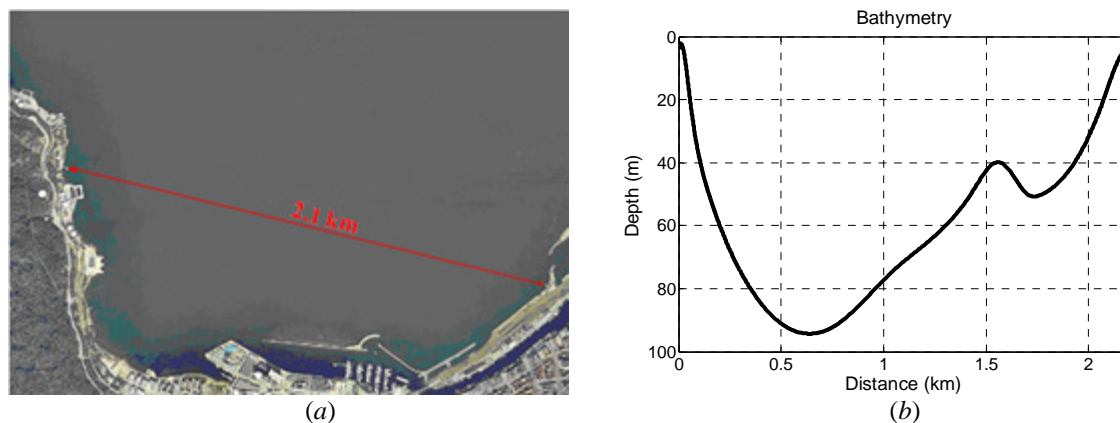


Figure 3. The trial location information and bathymetry

Figure 4 shows CIR estimations of RxA and RxB for one minute. CIR changes with time within 1 minute, and time delay spread is about 20 ms. Differently from results in Figure 2, there is no stable peak for detection, which is resulted from time-varying multipath, and arrival time of the strongest peaks in every cycle change within about 5 ms. The outputs from RxB have lower magnitudes than RxA, nearly one half. Without pre-knowledge of the multipath, receivers do not know the magnitude differences at different depths, so it is not reliable for them to make right decisions for acquisition. Though both RxA and RxB received signals at high SNRs, it is intractable to realize acquisition based on a fixed magnitude threshold, as there is no stable magnitude for detection within every match-filtering cycle.

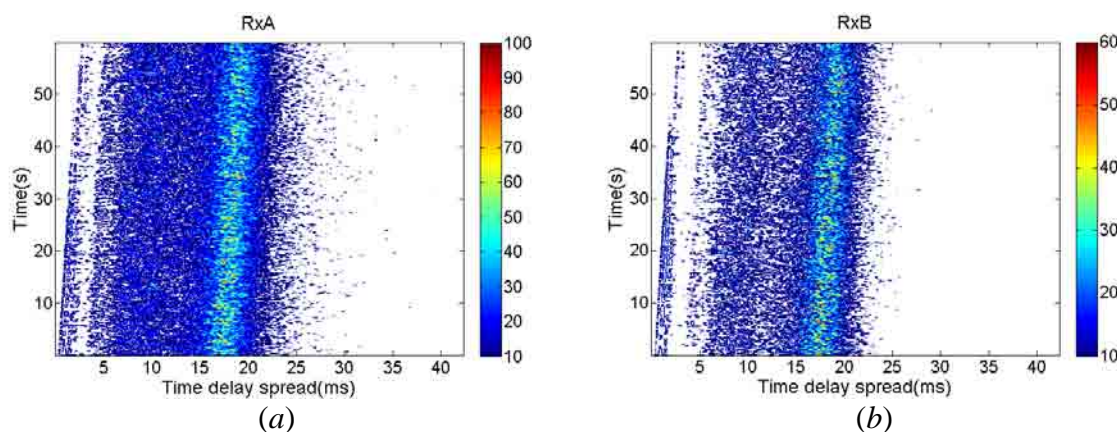


Figure 4. CIR estimations by replica correlation in 1 minute are shown in contour

The UWA multipath propagation is different from that in radio channel, and it mainly results from the reflections from two boundaries, a surface and a bottom. Refraction also influences propagation. If an experimental location is fixed, sound speed profile (SSP) still affects the multipath. SSP is sensitive to water temperature and salinity [9], and it changes with time. Ray tracing simulator developed by Jens M. Hovem [6] predicts ray tracks with given SSPs, and it can predict multipath with a plane ray model. In Figure 5, the acoustic ray tracks are shown. In those two months, SSPs were different mainly due to the difference of

water temperature, which is caused by the weather. In winter, most transmitted energy is constrained near the surface. It was proved in Figure 4, where RxA has higher magnitudes than RxB does since RxA was located near the surface. By predictions, multipath changes with time-varying SSP. For long term-deployed receivers, multipath change caused by SSP variation raises problems for the method of fixed magnitude detection.

From the experiments and analysis, difficulties for acquisition are analyzed. Match-filtering is optimal for deterministic signal detection, because it maximizes output SNR in presence of random noise [10]. It is not optimal in multipath, which is intractable to be predicted for receivers in advance. Magnitude detection of match-filtering is not reliable with a prefixed energy threshold in the reverberant multipath channel. The proposed design is to overcome difficulties of match-filtering in multipath channel.

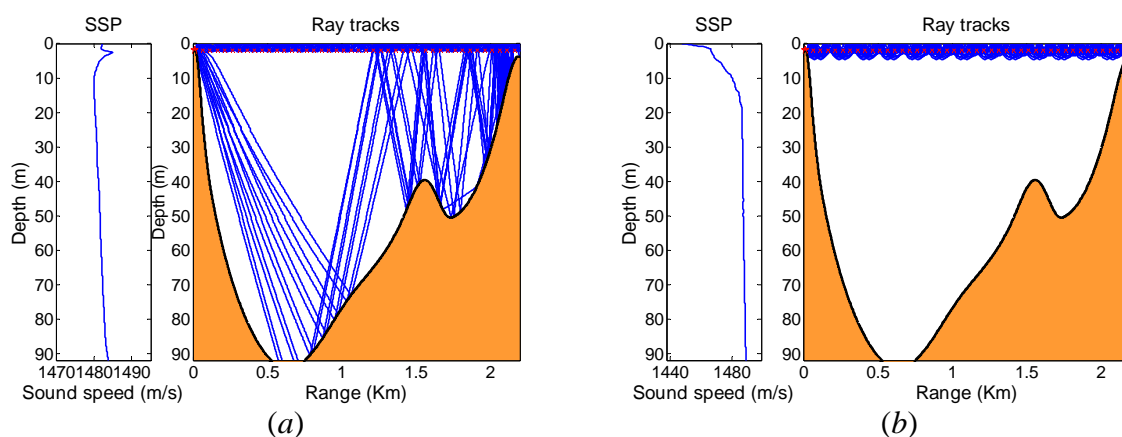


Figure 5. Ray tracing is conditioned by two different SSPs, and both SSPs were collected in Trondheim harbor. SSP in (a) was collected on April 4 2007, and SSP in (b) is collected on November 19 2007

2. FUNDAMENTALS OF PROPOSED DESIGN

An equalizer will be needed to mitigate the channel effects for acquisition [11], which applies adaptive signal processing to counter CIR, but it is computational intensive with many parameters. It is also sensitive to multipath parameter variations resulted from channel configurations, which is unpredictable in advance. The convergence of adaptive signal processing under changing channel conditions is difficult to be hold. The acquisition method based on adaptive equalizers has difficulties in realization for independent receivers powered by batteries.

Another method that could mitigate channel multipath is PPC, which uses a linear filter based on channel estimation by the probe signal [12–15] instead of adaptive filters. PPC is insensitive to slow oceanographic changes [15]. It produces a time focus with a great reduction of multipath by a vertical dense array, and this advantage makes it attractive for high rate underwater communication without inter-symbol interference. For point-to-point case with a single source and a single receiver, this idea can also be adopted by using a channel based linear filter in communication [12–14]. The received signal of one receiver can be modeled as

$$r_1(t) = h_1(t) \otimes s(t) + w_1(t), \quad (1)$$

where \otimes denotes convolution, $s(t)$ represents a sequence of communication symbols, $h_1(t)$ is the CIR of one receiver, and $w_1(t)$ is band-limited noise. PPC processing of the received signal in (1) is

$$\hat{r}_1(t) = h_1^*(-t) \otimes (h_1(t) \otimes s(t) + w_1(t)) = h_1^*(-t) \otimes h_1(t) \otimes s(t) + h_1^*(-t) \otimes w_1(t), \quad (2)$$

where the superscript $*$ denotes complex conjugate, and $w_1(t)$ is independent of $h_1^*(-t)$. In multipath propagation, different propagation paths are independent. $h_1^*(-t) \otimes h_1(t)$ is the auto-correlation of $h_1(t)$, the maximum value of which is coherent combining of the path gains, and side lobes of the auto-correlation depend on multipath distribution of $h_1(t)$. The maximum value of first term in (2) is larger than that of the second term, as $h_1(t)$ has no correlation with the noise.

In realization of PPC without an array, the received sequence of communication symbols is

$$r_s(t) = h_1(t) \otimes s_p(t) + w_1(t), \quad (3)$$

where $s_p(t) = s(t) \otimes p(t)$, and $p(t)$ is the transmitted probe signal. CIR is estimated by $p(t)$. The received probe signal is

$$r_p(t) = h_1'(t) \otimes p(t) + w_p(t), \quad (4)$$

where $w_p(t)$ is the band limited noise contaminating $p(t)$, and $h_1'(t)$ is CIR during $p(t)$ propagation. $r_p(t)$ acts as the channel estimation of $h_1(t)$ in (3), and the sequence of estimated symbols by PPC processing is

$$\hat{r}_1^p(t) = r_p^*(-t) \otimes r_s(t) = h_1'^*(-t) \otimes h_1(t) \otimes p^*(-t) \otimes p(t) \otimes s(t) + w_1(t) \otimes h_1'^*(-t) \otimes p^*(-t) + w_p^*(-t) \otimes h_1(t) \otimes s(t) \otimes p(t) + w_p^*(-t) \otimes w_1(t). \quad (5)$$

$w_p(t)$, $w_1(t)$, $p(t)$, and $h_1(t)$ are independent, so a coherent addition of the last three terms is small. Within coherence time, $h_1'(-t)$ is high correlated with $h_1(t)$. If $p(t)$ has a perfect auto-correlation property, for example the side lobes are zeros, and side lobes of $h_1'(-t) \otimes h_1(t)$ is suppressed. There is no waveform of the perfect auto-correlation property, but there are waveforms which approximate the property, such as LFM and maximum-length sequence.

PPC has immunity to complex CIR caused by multipath, and it is limited by temporal coherence, which is determined by relative movement between the transmitter and receiver. For example, $h_1'(-t)$ should high correlate with $h_1(t)$ in (5). Even at high input SNR, PPC will fail after a while. Because of variations, channel information $h_1'(-t)$ contained in the received probe signal loses correlation gradually with counterparts that are contained in the

later arriving signal. In stationary scenarios, the variation is mainly caused by a moving sea surface and time-varying oceanographic processes (see dilation effects in Figure 4), as the acoustic propagation speed is relative low. T. C. Yang [16] gives three methods to measure temporal coherence. One method is given by

$$\rho(t, \tau) = \frac{[r^*(-t) \otimes r(t + \tau)]_{\max}}{\sqrt{[r^*(-t) \otimes r(t)]_{\max} [r^*(-t - \tau) \otimes r(t + \tau)]_{\max}}}, \quad (6)$$

where $r(t) = s(t) \otimes h(t) + w(t)$ is the received signal, and it is contaminated by noise $w(t)$. $[r^*(-t) \otimes r(t + \tau)]_{\max}$ denotes the maximum value of convolution between the time reversed signal and the received signal after a time interval τ . The received periodical signal in the field trials can be used to measure temporal coherence.

Figure 6 gives temporal coherence measured in trials, and each point is a time averaged result in 1 minute. Temporal coherence declines with time increase. It decreases slower in the lake trial than that in the sea trial, and it is more than 0.9 within 1.6 second in Figure 6(a). In Figure 6(b), within 50 ms, temporal coherence is higher than 0.8, and there is no difference between RxA and RxB. There are differences between Figure 6(a) and Figure 6(b), as more is attributed to its lower frequency band in Figure 6(a) and the slow moving lake surface. Under the same channel configuration, Doppler spread is more distinct at a higher frequency band, for the Doppler shift is proportional to frequency as follow

$$f_d = \frac{fv}{c} \cos \theta, \quad (7)$$

where f_d is shift of frequency f due to relative movement at a speed of v , θ is the grazing angle, and c is sound speed. Coherence time t_c is defined by temporal coherence drop to 0.8 in [16], and it provides a reference for detection threshold for the design.

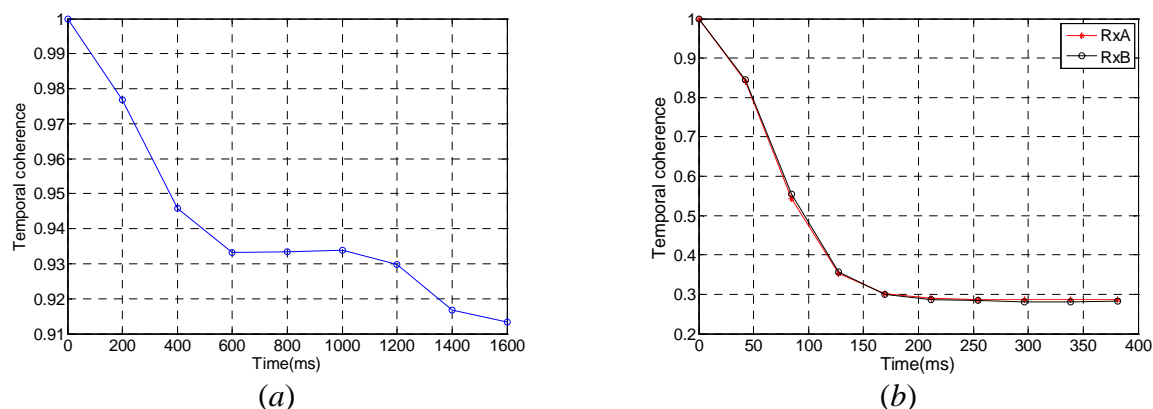


Figure 6. Temporal coherence measurements in lake trial (a) and sea trial (b)

The design is proposed to use two identical pulses of good auto-correlation for timing pulses, which are suitable for PPC processing in (5). The two pulses are separated by time t_w in order to keep off capturing late arrivals of the first pulse (Figure 7). t_w is known to the receiver. Correlation is often realized in frequency domain using FFT to cut computation load [17], so it is convenient for t_w to be the integer times of t_p . The receiver is motivated by PPC, and a detector makes a decision of detection by comparing the correlation coefficient between two pulses with a threshold. The coefficient detection metric is

$$\rho_M(t_w) = \frac{\left[\left| r_{p1}^*(-t) \otimes r_{p2}(t) \right| \right]_{\max}}{\sqrt{\int_{t_a}^{t_a+t_p} |r_{p1}(t)|^2 dt} \sqrt{\int_{t_a+2t_p+t_w}^{t_a+2t_p+t_w+t_p} |r_{p2}(t)|^2 dt}}, \tag{8}$$

where $r_{p1}(t)$ and $r_{p2}(t)$ are the two received pulses. If two identical pulses are transmitted within t_c , a high correlation coefficient between received signals can be achieved, which is indifferent to CIRs in the channel. The idea is to overcome the difficulty of acquisition in multipath channel. Monte Carlo simulation is carried out in white Gaussian noise channel without Doppler. The coefficients at different received SNRs are obtained in Figure 8. It is insensitive to SNR, as it fluctuates 3 dB when SNR changes from 0 dB and 20 dB

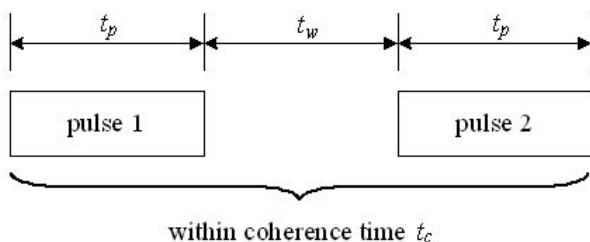


Figure 7.

Diagram for the timing pulses design

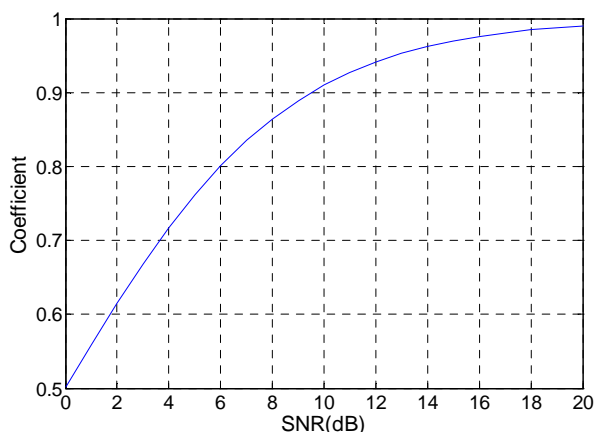


Figure 8.

Correlation coefficients under different SNRs

3. TRIAL VERIFICATION AND REALIZATION

In this design, PPC processing is adopted to overcome multipath, and a correlation coefficient between two pulses replaces magnitude threshold (or can be called as an energy threshold) for making a reliable decision of acquisition. In signal processing, the received probe signal is window clipped containing main paths' energy, which is required by PPC. From CIR estimations in Figure 2 and Figure 4, the time delay spreads are less than 100 ms and 42.3 ms respectively, so the clipping time length is one pulse time duration in each experiment. Figure 9 shows correlation coefficients between two continuous LFMs in the lake experiment. Stable output in 1 minute without multipath interference is obtained. Figure 10 shows correlation coefficients between two consecutive DSSS symbols in the sea experiment, there is no multipath problem. Both RxA and RxB have nearly the same results. Within t_c measured in Figure 6, the trials' results prove that the correlation coefficient between each pair pulses is stable and is not interfered from side lobes. It means that the coefficient is a better parameter for detection.

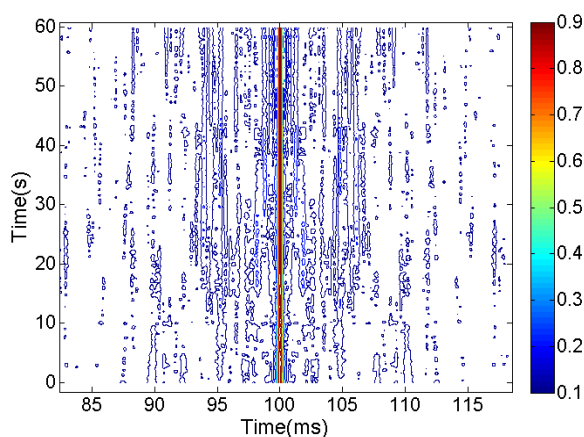


Figure 9.
Correlation coefficients ($t_w=100$ ms)

t_c determines the strength of correlation between two arrival pulses. It is difficult to know t_c in advance, for example in the stationary sea trial location in Trondheim harbor. Empirically, we can predict the maximum of t_c according to Doppler shift defined in (7). t_c is defined in [10] by

$$t_c = 1 / (4f_d). \quad (9)$$

Under the same channel configuration, the signal in a higher frequency band obtains shorter t_c , as it is sensitive to relative movement. In application, considerations are required to choose the parameters t_w and t_p , which are limited by t_c .

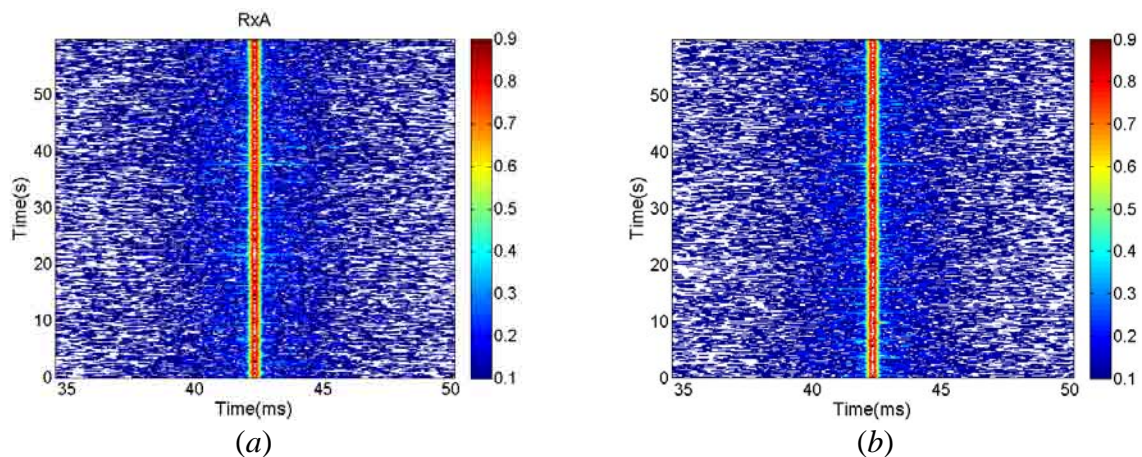


Figure 10. Correlation coefficients ($t_w=0$ ms)

Figure 11 gives the signal processing diagram for the receivers. There is no threshold to detect the first pulse. One replica correlator is utilized to iteratively match-filtering received signal, and updated probe is obtained by window clipping received signal in the current segment. The clipping depends on match-filtering, and it starts from the position of the maximum peak. The clipped signal serves for the second correlator, which carries out PPC processing for the detector. The second correlator computes the correlation coefficient between two pulses. Replica correlation is realized by overlap-save method (50 percent overlap is the most efficient) for fast convolution [17]. Discrete signal with a length of $2t_p$ is obtained in every FFT segment, and it is guaranteed that the updated signal with a length of t_p for PPC can be acquired. The probe signal has good auto-correlation, and it is ensured to catch a full length of received $p(t)$. If only a part of the first pulse in current FFT segment, the starting position of clipping is obtained randomly, as there is no correlation between full $p(t)$ and a part of $p(t)$. The updated probe signal is stored temporarily for t_w , and then it is discarded if a coefficient output is less than a threshold of the detector. The noises in different segments are independent, if the first pulse does not pass by the first correlator entirely, and a small coefficient is obtained by the second correlator. Based on the coefficient between one pair of identical transmitted pulses, the detector operates without interference from CIR.

According to the signal processing diagram, Figure 12 shows results of 300 pairs in the lake trial. Clipping length is 100 ms. The most of values are larger than 0.96, and only one is less than 0.90. Figure 13 shows results of 1471 pairs in the sea trial, where set t_w was set to zero in order to satisfy the limit of coherence time measured in Figure 6. Noticed reliable coefficient outputs, the most of values are larger than 0.80, and only one value of RxA is less than 0.70. Besides there is no difference between RxA and RxB, and it is different from the magnitude output in Figure 4, which overcomes the flaw of energy detection in reverberant multipath channel. In experiments, the processing produces stable coefficients along 1 minute, which are suitable for detection. The window clipping length of the received probe is important for PPC. Here it is not discussed how to optimize the T_{clip} , but this simple clipping method gets satisfied results in the experiments and is convenient for realization in signal processing.

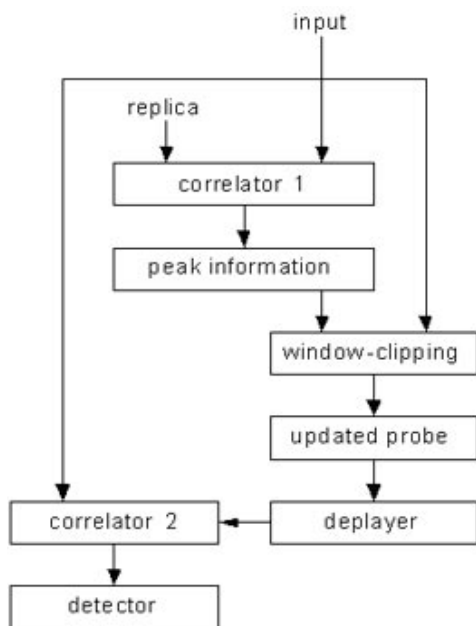
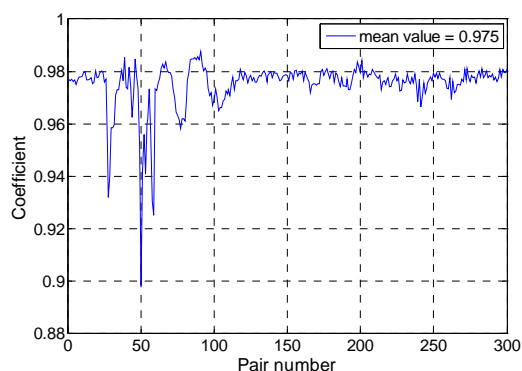
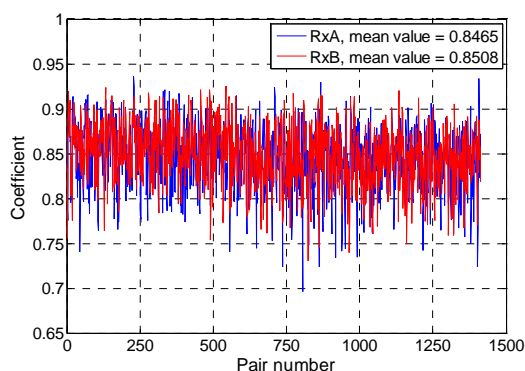


Figure 11.

The signal processing diagram for acquisition. The first correlator gives the peak information of maximum magnitude for window clipping in order to update the replica signal. The second correlator computes the correlation coefficients for detection

Figure 12. Output-coefficient ($t_w=100$ ms) in the lake trialFigure 13. Output-coefficient ($t_w=0$ ms) in the sea trial

CONCLUSIONS

Motivated by PPC, the proposed design solves a difficult problem for the acquisition of timing pulse in underwater reverberant multipath channel, it is simple without adaptive equalizers in realization, and only two correlators are used. Within coherence time, the correlation coefficient between two pulses is robust for detection. Coarse time synchronization can be achieved by this design, which does not depend on CIR or frequent threshold adjustments. Besides LFM and maximum-length sequences, other waveforms of good correlation could also be adopted, for example hyperbolic frequency modulation. In many underwater applications, this design has potential when time recovery is needed, especially for independent smart receivers, such as ranging transponders, communication receivers, and so on.

ACKNOWLEDGEMENTS

We give our great thanks for acoustic group of SINTEF ICT, Trondheim, who shares the access to the data collected for our analysis.

REFERENCES

1. A. Quazi and W. Konrad. Underwater acoustic communications. *IEEE Comm. Magazine*, pp. 24–29, Mar. 1982.
2. Xiaoyi Hu, Ru Xu, Wei Wei, Jing Liu, and Yongjun Xie. A novel scheme of timing synchronization For OFDM Underwater Communication System. *OCEANS 2008 MTS/IEEE Kobe Techno-Ocean*, pp. 1–5, Apr. 2008.
3. T. Schmidl and D. Cox. Robust frequency and timing synchronization for OFDM. *IEEE Trans. Comm.*, vol. 45, no.12, pp. 1613–1621, Dec. 1997.
4. US Patent 7218574. High range rate signaling.
5. J. G. Proakis. *Digital Communications*, NY: McGraw-Hill, 1995.
6. J. M. Hovem, Shefeng Yan, Xueshan Bao, and Hefeng Dong. Modeling underwater communication links. *The Second International Conference on Sensor Technologies and Applications*, 679–686, Aug., 2008.
7. W. G. MaMullen, B. A. Delaughe, and J. S. Bird. A simple rising-edge detector for time-of-arrival estimation. *IEEE Transactions on Instrumentation and Measurement*, vol. 45, no. 4, pp. 823–827, Aug. 1996.
8. Bayan S. Sharif, Jeff Neasham, Oliver R. Hinton, and Alan E. Adams. A computationally efficient Doppler compensation system for underwater acoustic communications. *IEEE J. Oceanic Eng.*, vol. 25, no. 1 pp. 52–61, Jan. 2000.
9. Finn B. Jensen, W. A. Kuperman, M. B. Porter, and Henrik Schmidt. *Computational Ocean Acoustics*. Springer-verlag, New York, 1992.
10. D. Tse and P. Viswanath. *Fundamentals of Wireless Communication*. Cambridge press, 2005.
11. M. Stojanovic and L. Freitag. Acquisition of direct sequence spread spectrum acoustic communication signals. *OCEANS 2003 Proceedings*, vol. 1, no. 2, pp. 279–286, 2003.
12. T. C. Yang and W. B. Yang. Performance analysis of direct-sequence spread spectrum underwater acoustic communications with low signal-to-noise ratio input signals. *J. Acoustic Soc. Am.* 123(2), pp. 842–855, Feb., 2008.
13. P. Hursky, M. B. Porter, J. A. Rice, and V. K. McDonald. Passive phase-conjugate signaling using pulse-position modulation. *OCEANS, 2001 MTS/IEEE Conference and Exhibition*, vol.4, pp. 2244–2249, 2001.
14. Paul Hursky, Michael B. Porter, and Martin Siderius. Point-to-point underwater acoustic communications using spread-spectrum passive phase conjugation. *J. Acoustic Soc. Am.* 120(1), 247–257, Jul., 2006.
15. W. A. Kuperman, William S. Hodgkiss, and Hee Chun Song. Phase conjugation in the ocean: Experimental demonstration of an acoustic time-reversal mirror. *J. Acoustic Soc. Am.* 103(1), 25–40, Jan., 1998.
16. T. C. Yang. Measurements of temporal coherence of sound transmissions through shallow water. *J. Acoustic Soc. Am.*, 120(5), pp. 2595–2164, Nov., 2006.
17. Alan V. Oppenheim and Ronald W. Schaffer. *Digital Signal Processing*. Prentice-hall.